SILICA COATINGS ON THE 1974 KILAUEA FLOW: NEW SEM AND SIMS RESULTS AND IMPLICATIONS FOR MARS. S. M. Chemtob[1], G. R. Rossman[1], J. M. Eiler[1], and B. L. Jolliff[2]. [1] California Institute of Technology, Pasadena, CA, 91125. (chemtob@gps.caltech.edu) [2] Washington University, St. Louis, MO.

Despite the predominately mafic character of martian surface rocks, silica-rich materials have long been predicted to occur on Mars [1]; recently, those predictions have been validated. CRISM spectra from numerous regions of Mars have revealed H_2O and OH^- bearing phases most consistent with amorphous silica [2]. Additionally, the detection of high-silica materials at Home Plate by MER Spirit implied aqueous alteration and leaching in a volcanic environment [3]. In order to fully understand the environments in which silica-rich materials are formed on Mars, it is useful to study silica in analogous terrestrial settings. We focus on silica and Fe-Ti oxide coatings in the Ka'u Desert on the island of Hawaii, an analog to Mars characterizeed by low levels of rainfall and strong acid-sulfate alteration processes [4]. Many formation mechanisms for these coatings have been proposed, including dissolution of wind-blown tephra [5], leaching of volcanic glass [6], and vapor deposition [7]. We focus on a suite of samples from the 1974 Kilauea pahoehoe flow, collected in 2003. The chemistry and morphology of these coatings were previously presented [8]. Here we present new morphological, spectral and isotopic analyses of the coating suite. The goal of the study is to characterize the coatings and their formation mechanism and describe the implications for silica mobility on Mars.

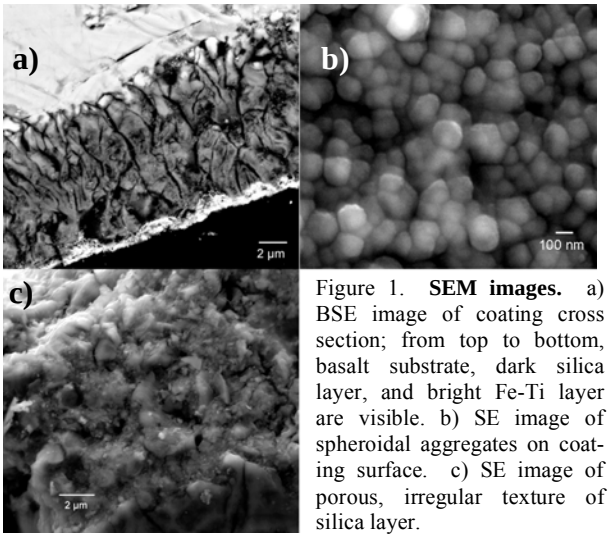

Figure 1. **SEM images.** a) BSE image of coating cross section; from top to bottom, basalt substrate, dark silica layer, and bright Fe-Ti layer are visible. b) SE image of spheroidal aggregates on coating surface. c) SE image of porous, irregular texture of silica layer.

Backscatter electron (BSE) and secondary electron (SE) images were collected with a LEO 1550 VP field emission SEM. Raman analyses were conducted using a Renishaw M1000 with a 514.5 nm Ar laser. Transmission infrared spectra were collected with a Magna-860 IR spectrometer, MCT-A detector and KBr beamsplitter. Oxygen isotope analyses were conducted on a Cameca 7f ion microprobe, with a primary Cs^+ beam focused to a 40 µm spot. Ti oxide isotopic standards were measured by laser fluorination (LFA) and analyzed on SIMS with the Hawaiian samples.

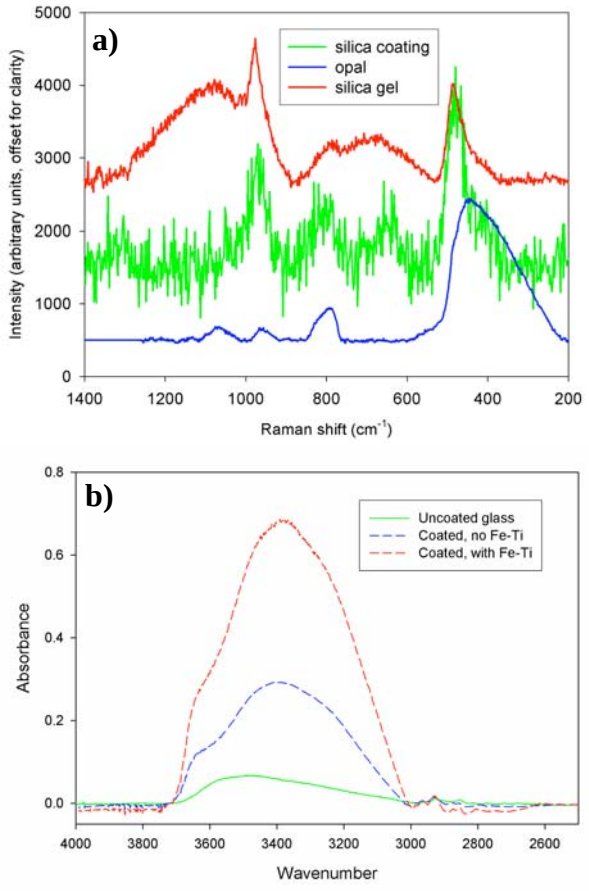

Figure 2. Spectral properties. a) Raman spectra of silica coating, with other silica phases for comparison. b) Transmission IR spectra of coating wafers, to determine water content.

Results: *Morphology and Chemistry*: As previously described, the coatings are composed of two distinct layers [8] (Fig. 1a). The lower coating layer, typically ~10 µm thick, is composed of amorphous silica, 93-100% SiO_2, with minor concentrations of Al_2O_3, MgO, FeO, and CaO. The silica-basalt boundary is sharp but undulating and appears to be made up of veins dissecting the glass surface. The upper coating layer, typically ~1 µm thick, is an Fe-Ti oxide with 75% TiO_2 and 20% FeO [8]. New SEM analyses indi-

cate that the upper coating surface appears to be an aggregate of spherules 50-150 nm in diameter (Fig. 1b). Spheroidal texture is commonly associated with depositional processes [9]. The silica material does not share this morphology and is observed instead to be blocky, angular and porous (Fig. 1c).

Spectral Properties: Previous Raman analyses revealed anatase as a dominant phase in the Fe-Ti coating [8]. Additional Raman analyses revealed rutile and other Fe-Ti oxides, such as armalcolite, may be present as microcrystals. Spectra of the silica layer are somewhat consistent with silica gel (Fig. 2a).

Transmission IR spectra were collected to determine water content of the coating materials. Using the value for ε_{water} in basalt from [10], the water content of the basaltic glass substrate was determined to be ~0.10 wt%. The transmission IR spectra of the coatings featured a broad peak centered at ~3370 cm^{-1} (Fig. 2b). Water content of the coating was determined to vary between 2-6.5 wt%. Higher water content was observed where the Fe-Ti coating was prominent.

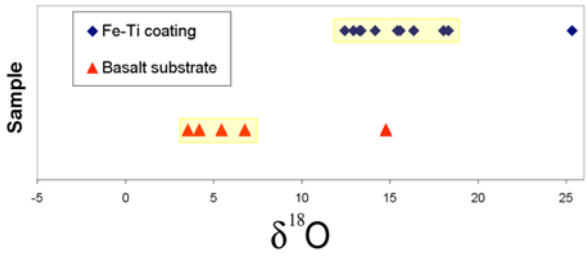

Figure 3. Oxygen isotope analyses. Both datasets feature a dominant modal value with one anomalous point. Yellow boxes mark the dominant values. The Fe-Ti layer is isotopically heavy compared to the basalt.

Isotopic Characteristics: Using LFA, $\delta^{18}O_{SMOW}$ of the basalt substrate was measured as 5.0±0.2‰, a value characteristic of Hawaiian glass. SIMS analyses of each natural coating surface were often highly variable, but featured a clear clustering of analyses (Fig. 3). Anomalous values may be explained by topography on the surface or genuine isotopic heterogeneity. The instrumental mass fractionations (IMF) were calculated based on measurements of standards. Ignoring highly anomalous points and using the mean of the clustered data, we determine $\delta^{18}O$ of the Fe-Ti coating to be 15.0±2.1‰.

The observation of enriched $\delta^{18}O$ does not distinguish between leaching and deposition mechanisms, but it does constrain the temperature of formation. Precipitation and groundwater $\delta^{18}O$ in the Ka'u Desert vary from -7.3 to -3.9‰ [11]. Using measured anatase-water fractionations [12], the maximum T to produce an equilibrium fractionation of the magnitude observed is ~253 K, an unreasonably low value. Therefore, the coating could not have been deposited hot in equilibrium with regional waters; some kinetic fractionation, possibly related to evaporation, must have occurred.

Discussion: Our observations indicate a multiple-step formation mechanism. The glassy morphology, Raman spectral signature and enriched $\delta^{18}O$ of the silica coating suggest it is a residual product of acid-sulfate alteration. This is consistent with the findings of recent studies of similar materials [6]. However, the spheroidal texture of the Fe-Ti coating requires transportation and redeposition of those materials out of solution. Fe and Ti were released into solution by chemical weathering of basaltic glass or accessory phases such as titanomagnetite [13]. NanoSIMS maps with an O^- beam source showed enhanced concentrations of F and Cl in the outer coating, suggesting Ti may have been transported in soluble halide complexes such as TiF_6^{2-}. The outer coating was then deposited from an evaporating solution at low T. The characteristic transport distance associated with these materials is not yet known.

The Hawaiian coating chemistry bears a striking resemblance to the deposits unearthed at Gusev Crater: enriched in Si and Ti but depleted in Al [3]. This suggests that both deposits are the result of volcanically derived acid-sulfate alteration. A major difference between the two is the volume of alteration; the Ka'u Desert coatings are a surface phenomenon, whereas the Gusev rocks are volume-altered. The degree of alteration observed may be a function of time and intensity of alteration; similarly volume-altered basalts can be found in Hawaii near long-active fumaroles [14]. Therefore, the silica-rich rocks at Gusev may have been exposed to acidic aqueous alteration for extended periods of time. The extent of alteration within orbitally detected silica-bearing strata is unknown [2]. Further textural and geochemical analyses of high-silica terrestrial analogs will provide further insight on past aqueous weathering processes on the martian surface.

Acknowledgements: Support from NASA grant NNX06AB20G (GRR) is appreciated. We thank C. Ma and Y. Guan for help in the SEM and SIMS labs.

References: [1] McLennan (2003) *Geology*, **31**, 315 [2] Milliken et al. (2008) *Geology*, **36**, 847 [3] Squyres et al. (2008), *Science*, **320**, 1063 [4] Seelos et al., in prep. [5] Curtiss et al. (1985) *GCA*, **49**, 49 [6] Minitti et al. (2007) *JGR*, **112**, 10.1029/2006JE002839 [7] Schiffman et al. (2006) *Geology*, **34**, 921. [8] Chemtob et al. (2006) *LPSC 37*, #1443. [9] Rodgers et al. (2002) *Clay Min.*, **37**, 299 [10] Stolper (1982) *Contrib. Min. Pet.*, **81**, 1. [11] Scholl et al. (1995) USGS 95-4213. [12] Bird et al. (1993) *GCA*, **57**, 3083. [13] Arlauckas and McLennan, *LPSC 36*, #2011. [14] Morris et al. (2000) *LPSC 31*, #2014.